Truncated V2 Vasopressin Receptors as Negative Regulators of Wild-Type V2 Receptor Function

Xiangyang Zhu and Jürgen Wess*

Laboratory of Bioorganic Chemistry, NIDDK, National Institutes of Health, Bethesda, Maryland 20892

Received May 18, 1998; Revised Manuscript Received August 14, 1998

ABSTRACT: Accumulating evidence suggests that G protein-coupled receptors (GPCRs) can form dimeric or oligomeric arrays. Based on this concept, we have tested the hypothesis that truncated GPCRs can act as negative regulators of wild-type receptor function. Using the G_S-coupled V2 vasopressin receptor as a model system, we systematically analyzed the ability of N- and C-terminal V2 receptor fragments to interfere with the activity of the wild-type V2 receptor coexpressed in COS-7 cells. Several N-terminal V2 receptor truncation mutants were identified that strongly inhibited the function (as determined in cAMP and radioligand binding assays) and cell surface trafficking of the coexpressed full-length V2 receptor. However, these truncation mutants did not interfere with the function of other G_S-coupled receptors such as the D1 dopamine and the β2-adrenergic receptors. Dominant negative effects were only observed with mutant receptors that contained at least three transmembrane domains. In addition, immunoblotting experiments showed that all V2 receptor truncation mutants displaying dominant negative activity (but not those mutant receptors lacking this activity) were able to form heterodimers with the full-length V2 receptor, suggesting that complex formation between mutant and wild-type V2 receptors underlies the observed inhibition of wild-type receptor function. Given the high degree of structural homology shared by all GPCRs, our findings should also be applicable to other members of this receptor superfamily.

All members of the superfamily of G protein-coupled receptors (GPCRs)[1] are predicted to share a similar molecular architecture characterized by the presence of seven transmembrane helices (TM I−VII) that are connected by three intracellular (i1−i3) and three extracellular loops (o1−o3; Figure 1) (*1*−*3*). Models describing the interaction of GPCRs with their G protein targets are generally based on the assumption that the receptors exist as monomers and couple to G proteins in an 1:1 stoichiometry. However, several recent studies suggest that such classical models of receptor/G protein coupling may be oversimplified.

Pharmacological studies, for example, have shown that the complex agonist binding properties of muscarinic acetylcholine receptors can be explained best by postulating cooperativity among receptor proteins arranged in oligomeric complexes (*4*−*7*). A similar conclusion has been reached based on genetic complementation experiments involving the coexpression of two different, functionally active mutant GPCRs (*8, 9*). Monnot et al. (*9*), for example, recently described two angiotensin II mutant receptors which, when expressed alone, did not show any ligand binding activity. However, upon coexpression of the two receptor constructs, ligand binding activity was restored, probably due to protein trans-complementation (*9*).

The concept that GPCRs can exist as oligomers is also strongly supported by several recent studies examining receptor expression via immunological techniques. Immunoblotting experiments with different GPCRs have shown that GPCRs are able to form SDS-resistant dimers or multimers (for recent studies, see refs *10*−*15*). Furthermore, a recent immunoprecipitation study employing receptor constructs carrying different epitope tags demonstrated that β2-adrenergic receptors exist in dimeric forms (*10*). These investigators also provided evidence that the formation of receptor dimers is not an artifact of membrane preparation or solubilization and is critical for efficient G protein activation (*10*). In addition, dimer formation was found to be receptor-specific (β2-adrenergic and m2 muscarinic receptors, for example, did not form heterodimers), excluding the possibility that the receptor dimers or oligomers simply represent nonspecific aggregates (*10*).

Coexpression studies with 'split' GPCRs have demonstrated that GPCRs can be assembled from multiple, independently stable receptor fragments (*16*−*21*). For example, when the G_S-coupled V2 vasopressin receptor was split in the i3 loop, COS-7 cells cotransfected with the two receptor fragments (referred to as Ni3 and V2-tail; Figure 1) were able to respond to ligand stimulation with a pronounced increase in cAMP production (*21*). In addition, evidence was provided that functionally inactive mutant V2 vasopressin [occurring in patients with X-linked nephrogenic

* To whom correspondence should be addressed: National Institute of Diabetes and Digestive and Kidney Diseases, Laboratory of Bioorganic Chemistry, Bldg. 8A, Rm. B1A-05, Bethesda, MD 20892. Telephone: 301-402-3589. Fax: 301-402-4182. E-mail: jwess@helix.nih.gov.

[1] Abbreviations: AVP, [Arg^8]vasopressin; DMEM, Dulbecco's modified Eagle's medium; DTT, dithiothreitol; ELISA, enzyme-linked immunosorbent assay; FBS, fetal bovine serum; GPCRs, G protein-coupled receptors; HA tag, hemagglutinin epitope tag; i1−i3, the three intracellular loops of GPCRs; NDI, nephrogenic diabetes insipidus; o1−o3, the three extracellular loops of GPCRs; PBS, phosphate-buffered saline; PCR, polymerase chain reaction; PMSF, phenylmethanesulfonyl fluoride; TM I−VII, the seven transmembrane domains of GPCRs.

10.1021/bi981162z
Published on Web 10/23/1998

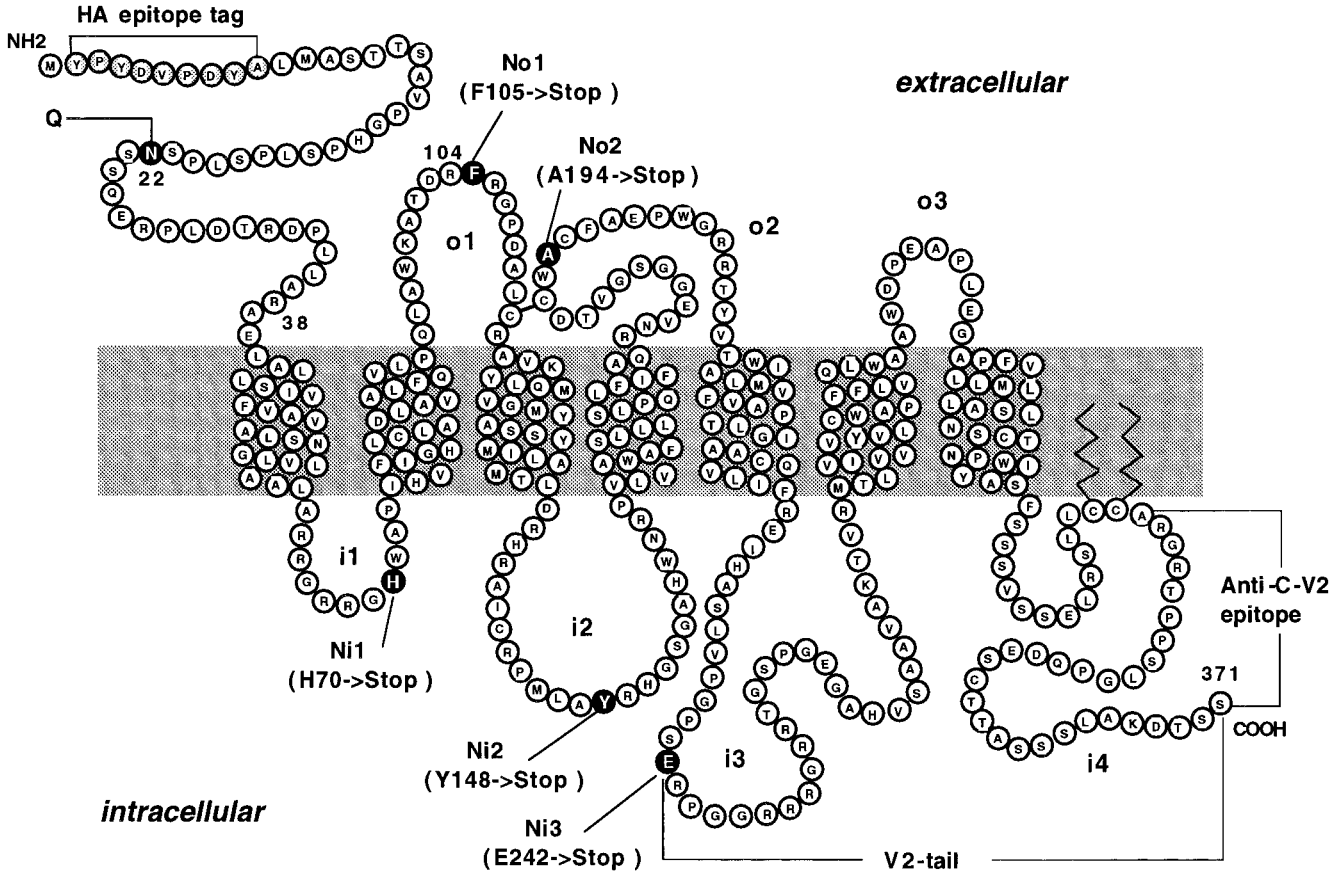

FIGURE 1: Schematic representation of the human V2 vasopressin receptor indicating the structure of mutant V2 receptors analyzed in this study. The three intracellular and three extracellular loops are referred to as i1−i3 and o1−o3, respectively. To generate a series of truncated V2 receptors, the indicated amino acid codons (His70, Phe105, Tyr148, Ala194, and Glu242) were replaced with translation termination codons, resulting in Ni1, No1, Ni2, No2, and Ni3, respectively. To create a mutant V2 vasopressin receptor that is no longer a substrate for N-linked glycosylation, Asn22 was replaced with Gln (*27*). To allow translation of the C-terminal V2-tail polypeptide (Glu242−Ser371), an ATG start codon was placed immediately upstream of the Glu242 codon (*21*). The nine amino acid N-terminal HA epitope tag present in all receptor constructs is highlighted. A rabbit polyclonal antibody (referred to as anti-C-V2) was raised against the indicated C-terminal receptor sequence. Numbers refer to amino acid positions in the human V2 vasopressin receptor sequence (*22*).

diabetes insipidus (NDI)] can be functionally rescued (fully or partially) by coexpression with the V2-tail polypeptide spanning the region where various mutations occur (*21*).

On the basis of these findings, we hypothesized that it should also be possible to identify mutant V2 receptors that are able to interfere with the function of the wild-type V2 receptor via complex formation. We initially showed, using cotransfected COS-7 cells, that the Ni3 V2 receptor truncation mutant but not the V2-tail polypeptide can interfere with the ability of the wild-type V2 receptor to bind ligands and to properly couple to G proteins. To further explore the structural basis underlying the dominant negative activity of the Ni3 mutant receptor, we next generated a series of additional V2 mutant receptors that had been truncatd in the i1, o1, i2, and o2 loops (Figure 1). Coexpression studies demonstrated that only those mutant receptors that contained the first three TM domains (TM I−III) were able to act as negative regulators of wild-type receptor function.

In addition, the molecular mechanism by which truncated V2 receptors interfere with wild-type receptor function was further explored by studying receptor cell surface localization via ELISA using wild-type and mutant receptor constructs carrying an N-terminal hemagglutinin (HA) epitope tag. Moreover, immunoblotting experiments were carried out to study complex formation between wild-type and mutant receptors. We found that expression of all mutant receptors displaying dominant negative activity (but not of those unable to interfere with wild-type receptor function) led to greatly reduced cell surface expression of the wild-type receptor protein and to the formation of heterodimeric complexes with the full-length V2 receptor. These results provide novel insight into the molecular basis of GPCR function.

EXPERIMENTAL PROCEDURES

DNA Constructs. All mutations were introduced into V2pcD-PS (*21*), a mammalian expression vector coding for the human V2 vasopressin receptor (*22*), using standard polymerase chain reaction (PCR) mutagenesis techniques (*23*). All wild-type and truncated mutant receptor constructs contained a nine-amino acid HA epitope tag (YPYDVPDYA; *24*) inserted after the initiating methionine codon. The ligand binding and G protein-coupling properties of the epitope-tagged wild-type V2 receptor did not differ significantly from those found with the non-tagged version (*21*, *25*). For the construction of truncated V2 vasopressin receptors (referred to as Ni1, No1, Ni2, No2, and Ni3; Figure 1), stop codons (TGA) were inserted at the appropriate positions in V2pcD-PS. The stop codons were placed approximately in the center of the i1, o1, i2, and o2 loops. The Ni3 (Glu242→stop) fragment (truncation within the i3 loop) was generated since

this mutant receptor has been identified in NDI patients (*26*). In addition, an expression plasmid was created in which amino acids Arg38−Arg104 were deleted from Ni3, resulting in V2(III−V). No other N-terminal V2 receptor fragments were generated. The construction of an expression vector coding for the C-terminal V2-tail polypeptide (Glu242−Ser371; Figure 1) has been described previously (*21*). To generate a plasmid coding for a glycosylation-defective V2 receptor (*27*), a 143-base pair synthetic *Eco*RI−*Nhe*I fragment encoding an Asn22→Gln point mutation was used to replace the corresponding sequence in V2pcD-PS.

The construction of expression plasmids coding for the m3-Ni3 and m3-tail mutant receptors has been described previously (*17*). m3-Ni3 and m3-tail are receptor fragments derived from the rat m3 muscarinic receptor (Glu273→stop and Leu388−Leu589, respectively) and are structurally homologous to the Ni3 and V2-tail V2 receptor polypeptides, respectively (Figure 1). In addition, the following wild-type receptor expression plasmids were used: human D1 dopamine receptor (*28*) in pcDNAI, rat β2-adrenergic receptor (*29*) in pSVL, and rat V1a vasopressin receptor (*30*) in pcD-SP6/T7. The identity of the various constructs and the correctness of all PCR-derived sequences were verified by restriction endonuclease analysis and by dideoxy sequencing of the mutant plasmids.

Transient Expression of Wild-Type and Mutant V2 Receptors. COS-7 cells were grown in Dulbecco's modified Eagle's medium (DMEM) containing 10% fetal bovine serum (FBS) at 37 °C in a humidified 5% CO_2 incubator. For transfections, 2×10^6 cells were seeded into 100-mm dishes. About 24 h later, cells were transfected with the various receptor constructs (4 μg of plasmid DNA per dish) by a DEAE−dextran method (*31*). In cotransfection experiments, the total amount of transfected DNA was kept constant at 4 μg per dish.

Radioligand Binding Assays. For radioligand binding studies, COS-7 cells were harvested approximately 72 h after transfections, and membrane homogenates were prepared as described (*32*). Binding buffer consisted of 50 mM Tris (pH 7.4), 3 mM $MgCl_2$, 1 mM EDTA, 0.1% bovine serum albumin, and 0.1 mg/mL bacitracin. Incubations were carried out for 1 h at room temperature in a 0.5 mL volume with 2 nM radioligand, [^{3}H]arginine vasopressin ([^{3}H]AVP, 81 Ci/mmol; Dupont NEN). For saturation binding studies, six different concentrations of [^{3}H]AVP (0.125−4 nM) were used. Nonspecific binding was assessed in the presence of 5 μM AVP. Protein concentrations were determined according to Bradford (*33*). Binding data were analyzed by a nonlinear least squares curve-fitting procedure using the computer program LIGAND (*34*).

cAMP Assays. Approximately 20−24 h after transfections, COS-7 cells were transferred into 6-well plates, and 2 μCi/mL of [^{3}H]adenine (15 Ci/mmol; American Radiolabeled Chemicals Inc.) was added to the growth medium. After a 40−48 h labeling period, cells were preincubated in Hanks' balanced salt solution containing 20 mM Hepes and 1 mM 3-isobutyl-1-methylxanthine for 15 min (37 °C) and then stimulated with 1 μM AVP for 30 min at 37 °C. To generate complete concentration−response curves, six different concentrations of AVP (ranging from 10^{-13} to 10^{-5} M) were used. Incubations were terminated by aspiration of medium and addition of 1 mL ice-cold 5% trichloroacetic acid containing 1 mM ATP and 1 mM cAMP. Increases in intracellular [^{3}H]cAMP levels were determined by anion exchange chromatography as described (*21, 35*).

ELISA. An indirect cellular ELISA was performed to quantitate the amount of epitope-tagged wild-type and mutant V2 receptor proteins present on the cell surface (*18, 21*). COS-7 cells were transferred into 96-well plates ($4-5 \times 10^4$ cells/well) about 24 h after transfections. Approximately 48 h later, cells were fixed with 4% formaldehyde in phosphate-buffered saline (PBS) for 30 min at room temperature. After being washed with PBS and blocked with DMEM containing 10% FBS, cells were incubated for 2 h at 37 °C with a monoclonal antibody directed against the HA epitope tag (12CA5, Boehringer Mannheim; 10 μg/mL in DMEM, 10% FBS). Plates were then washed and incubated with 1:2000 dilution (in DMEM containing 10% FBS) of a horseradish peroxidase-conjugated goat anti-mouse IgG antibody (Sigma) for 1 h at 37 °C. Subsequently, H_2O_2 and *o*-phenylenediamine (2.5 mM each in 0.1 M phosphate−citrate buffer, pH 5.0) were added to serve as substrate and chromogen, respectively. Enzymatic reactions (carried out at room temperature) were stopped after 10 min with 1 M H_2SO_4 solution containing 0.05 M Na_2SO_3, and color development was measured bichromatically in the Biokinetics reader (EL 312, Bio Tek Instruments, Inc., Winooski, VT) at 490 and 630 nm.

Preparation of Membrane Lysates. For Western blotting experiments, membrane extracts were prepared from transfected COS-7 cells as follows. About 70−72 h after transfections, cells were scraped into ice-cold PBS, transferred into Eppendorf tubes, and centrifuged at 2000 rpm for 5 min in a microcentrifuge. Supernatants were discarded, and cell pellets were resuspended in 200 μL of PBS containing 0.2% digitonin, 1 mM phenylmethanesulfonyl fluoride (PMSF, Sigma), and 1 μg/mL pepstatin A (Sigma) to remove soluble proteins as well as peripheral membrane proteins. After incubation on ice for 20 min, cell pellets were collected by centrifugation at 2500 rpm for 5 min, followed by incubation with 200 μL of lysis buffer (PBS containing 1% digitonin, 0.5% deoxycholate, 1 mM PMSF, and 1 μg/mL pepstatin A) at 4 °C for 1 h. Subsequently, cell lysates were centrifuged in a refrigerated Eppendorf 5417R microcentrifuge at maximal speed for 30 min. Supernatants were used either immediately for Western blotting or stored at −80 °C prior to use.

Western Blotting. Membrane lysates prepared from transfected COS-7 cells were mixed with 3 × nonreducing Laemmli sample buffer (Bio-Rad Laboratories). To allow for reducing conditions, samples were incubated with 100 mM DTT (final concentration) for 30 min at room temperature or heated (in the presence of 100 mM DTT) at 95 °C for 3 min prior to SDS−PAGE. Subsequently, samples were resolved on 10−15% (w/v) acrylamide slab gels in the presence of 0.1% SDS. For immunoblotting experiments, proteins were transferred to nitrocellulose membranes and probed with either the anti-HA 12C5A mouse monoclonal antibody (1 μg/mL) or the anti-C-V2 rabbit polyclonal antibody (1 μg/mL; kindly provided by Dr. Paul Goldsmith, NIH) raised against a peptide corresponding to the C-terminal 29 amino acids of the human V2 vasopressin receptor (Figure 1). Bound antibody was then detected with a secondary antibody (goat anti-mouse or monkey anti-rabbit, respec-

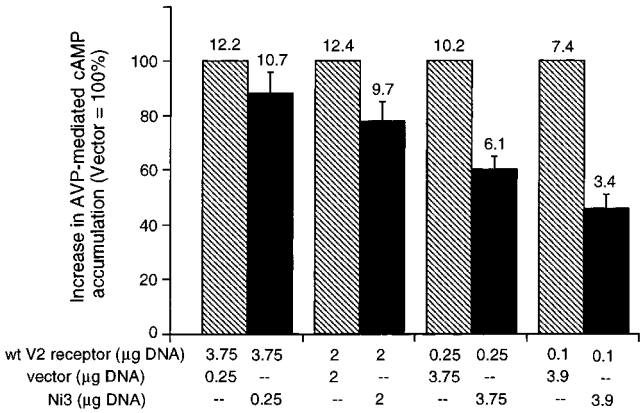

FIGURE 2: Inhibition of wild-type V2 receptor-mediated cAMP accumulation by the Ni3 truncation mutant. COS-7 cells were cotransfected with the indicated amounts of plasmid DNA coding for the wild-type V2 receptor and the Ni3 V2 receptor truncation mutant or pcD-PS vector DNA (control). The structure of the Ni3 construct is given in Figure 1. Cells were incubated in 6-well plates for 30 min (at 37 °C) in the absence or presence of 1 μM AVP. The resulting increases in intracellular cAMP levels (fold stimulation above basal) were determined as described under Experimental Procedures. In each individual experiment, cAMP responses observed with vector-cotransfected control cells were set equal to 100%. Numbers above bars indicate actual increases in cAMP levels (fold stimulation above basal level; means). Data are given as means ± SE of at least three independent experiments, each carried out in triplicate.

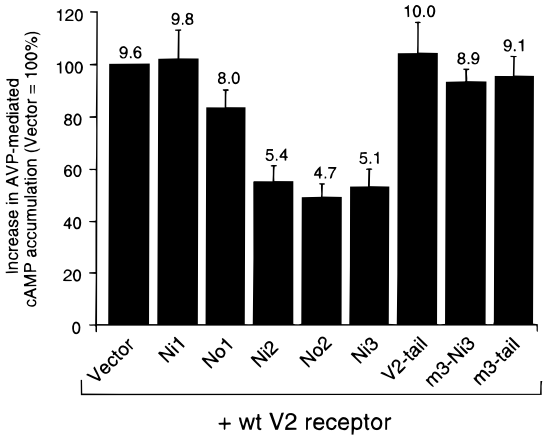

FIGURE 3: Inhibition of wild-type V2 receptor-mediated cAMP production by truncated V2 receptors. COS-7 cells were cotransfected with plasmid DNA coding for the wild-type V2 receptor (0.25 μg) and the indicated mutant receptor constructs or pcD-PS vector DNA (3.75 μg each). The structures of the different mutant receptors/receptor fragments are given in Figure 1 and under Experimental Procedures. The m3-Ni3 and m3-tail polypeptides are derived from the rat m3 muscarinic receptor (*17*) and are structurally homologous to Ni3 and V2-tail, respectively. Cells were incubated in 6-well plates for 30 min (at 37 °C) in the absence or presence of 1 μM AVP. The resulting increases in intracellular cAMP levels (fold stimulation above basal) were determined as described under Experimental Procedures. In each individual experiment, cAMP responses observed with vector-cotransfected control cells were set equal to 100%. Numbers above bars indicate actual increases in cAMP levles (fold stimulation above basal level; means). Data are given as means ± SE of at least three independent experiments, each carried out in triplicate.

tively) conjugated to horseradish peroxidase, using an enhanced chemiluminescence detection kit (Amersham).

RESULTS

Constructs. A series of truncated V2 vasopressin receptors were created by introducing translation stop codons into the i1, o1, i2, o2, and i3 loops. These mutant receptors were designated Ni1 (His70→stop), No1 (Phe105→stop), Ni2 (Tyr148→stop), No2 (Ala194→stop), and Ni3 (Glu242→stop), respectively (Figure 1). To allow for the detection of wild-type and mutant receptor proteins via immunological techniques, a nine amino acid HA epitope was added to the N-terminus of all constructs (Figure 1). Previous studies showed that the presence of the epitope tag had no significant effect on the ligand binding and G protein-coupling properties of the wild-type V2 receptor (*21*, *25*). Upon transient expression in COS-7 cells, the different V2 receptor truncation mutants were unable to bind the radioligand, [^{3}H]AVP, or to stimulate AVP-dependent increases in cAMP levels (data not shown).

Inhibition of V2 Vasopressin Receptor Signaling by Coexpressed Truncated V2 Receptors. We first wanted to study whether coexpressed V2 receptor truncation mutants were able to impair wild-type V2 receptor function in cotransfected COS-7 cells. Initially, we examined the ability of the Ni3 mutant receptor (obtained by 'splitting' the V2 receptor within the i3 loop; *21*) to interfere with wild-type V2 receptor-mediated increases in cAMP production. Toward this goal, different amounts (0.25−3.9 μg) of Ni3 construct or pcD-PS vector DNA (as control) were cotransfected with wild-type V2 receptor DNA, keeping the total amount of transfected DNA constant at 4 μg. As shown in Figure 2, increasing the amount of cotransfected vector DNA led to progressive reductions in maximum cAMP responses (from 12- to 7-fold above basal) induced by ligand stimulation (1 μM AVP) of the wild-type V2 receptor. This effect is most probably due to competition between receptor and vector DNA for amplification in COS-7 cells. However, compared to the responses seen with vector-cotransfected cells (which were set equal to 100% in each individual experiment), cAMP responses observed with cells coexpressing the Ni3 fragment and the wild-type V2 receptor were significantly reduced. Figure 2 shows that expression of the Ni3 mutant receptor led to concentration-dependent reductions in maximum cAMP responses. For example, increasing the amount of cotransfected Ni3 DNA from 2 to 3.75 μg led to an inibition of cAMP responses by approximately 20 and 40%, respectively.

We next wanted to define the minimum structural requirements for the ability of the Ni3 mutant receptor to interfere with wild-type receptor signaling. Thus, additional cotransfection experiments were carried out with progressively shortened V2 receptor truncation mutants (Ni1, No1, Ni2, and Ni2; Figure 1). Based on the initial findings obtained with the Ni3 fragment, we decided to use a fixed ratio of mutant V2 receptor or vector DNA (3.75 μg) and wild-type V2 receptor plasmid (0.25 μg) in all further experiments. As shown in Figure 3, little or no inhibition of AVP-induced cAMP responses was seen in the presence of the coexpressed Ni1 and No1 fragments. Similar findings were obtained when the C-terminal V2 receptor polypeptide, V2-tail (Figure 1), was coexpressed with the full-length V2 receptor (Figure 3). In contrast, the Ni2 and No2 fragments were able to interfere with wild-type V2 receptor signaling in a fashion similar to the Ni3 mutant receptor, leading to reductions in AVP-stimulated cAMP levels by approximately 50% (Figure 3). However, complete AVP concentration−response curves

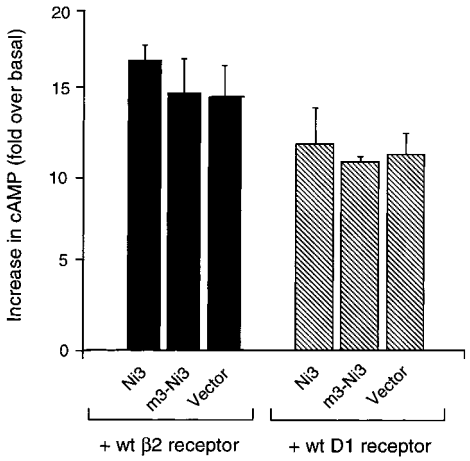

FIGURE 4: Lack of inhibition of D1 dopamine and β2-adrenergic receptor-mediated cAMP accumulation by the Ni3 V2 receptor truncation mutant. COS-7 cells were cotransfected with plasmid DNA coding for the wild-type human D1 dopamine or rat β2-adrenergic receptors (0.25 μg each) and the Ni3 V2 receptor truncation mutant, the m3-Ni3 mutant muscarinic receptor construct, or pcD-PS vector DNA (3.75 μg each). Cells were incubated in 6-well plates for 30 min (at 37 °C) in the absence or presence of 1 mM dopamine (D1 dopamine receptor) or 0.2 mM (−)-isoproterenol (β2-adrenergic receptor). The resulting increases in intracellular cAMP levels (fold stimulation above basal) were determined as described under Experimental Procedures. Data are given as means ± SE of three independent experiments, each carried out in triplicate.

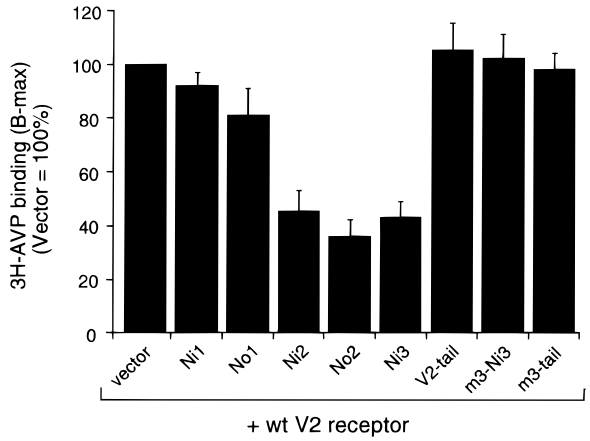

FIGURE 5: Inhibition of radioligand binding to the wild-type V2 receptor by coexpressed truncated V2 receptors. COS-7 cells were cotransfected with plasmid DNA coding for the wild-type V2 receptor (0.25 μg) and the indicated mutant receptor constructs or pcD-PS vector DNA (3.75 μg each). The structures of the different mutant receptors/receptor fragments are given in Figure 1 and under Experimental Procedures. The m3-Ni3 and m3-tail polypeptides are derived from the rat m3 muscarinic receptor (*17*) and are structurally homologous to Ni3 and V2-tail, respectively. [^{3}H]AVP binding studies were carried out with membrane homogenates prepared from cotransfected COS-7 cells as described under Experimental Procedures. Data are given as means ± SE of at least three independent experiments, each carried out in duplicate.

showed that the coexpressed Ni2, No2, and Ni3 mutant receptors had no significant effect on AVP EC_{50} values (data not shown; AVP EC_{50} in vector-cotransfected control cells: 0.30 ± 0.04 nM).

To examine whether the observed inhibition of V2 receptor-mediated functional responses was specific for V2 receptor fragments, the wild-type V2 receptor was also coexpressed with a truncated rat m3 muscarinic receptor, m3-Ni3 (Glu273→stop; *17*), which is structurally homologous to the Ni3 V2 mutant receptor. However, as shown in Figure 3, the coexpressed m3-Ni3 receptor had no significant effect on V2 receptor-mediated increases in adenylyl cyclase activity. Similar results were obtained when the wild-type V2 receptor was coexpressed with a C-terminal m3 muscarinic receptor fragment (m3-tail; Leu388−Leu589; *17*) that is structurally homologous to the V2-tail polypeptide.

Truncated V2 Receptors Do Not Interfere with the Function of Other G_S-Coupled Receptors. We next wanted to exclude the possibility that the ability of the Ni2, No2, and Ni3 mutant receptors to interfere with wild-type V2 receptor function occurred via sequestration of the stimulatory G protein, G_s. We therefore studied the ability of the Ni3 fragment to affect signaling induced by two other G_s-coupled receptors, the human D1 dopamine (*28*) and the rat β2-adrenergic receptors (*29*). Control experiments with vector-cotransfected cells showed that the D1 dopamine and β2-adrenergic receptors were able to mediate pronounced increases in intracellular cAMP levels (10−17-fold above basal) when stimulated by the appropriate agonist ligands [1 mM dopamine and 0.2 mM (−)-isoproterenol, respectively] (Figure 4). As shown in Figure 4, maximum cAMP responses obtained in the presence of the coexpressed Ni3 V2 mutant receptor were not significantly different from those found with vector-cotransfected control cells. Similar results were obtained with cells coexpressing the D1 dopamine or the β2-adrenergic receptor and the m3-Ni3 mutant receptor, which is structurally homologous to the Ni3 mutant V2 receptor construct (Figure 4). These data indicate that the ability of the Ni3 fragment and, most likely, other V2 receptor truncation mutants to interfere with wild-type V2 receptor function is not due to competition at the G protein level.

Truncated V2 Receptors Reduce Ligand Binding to the Wild-Type V2 Receptor. We next wanted to examine whether coexpressed V2 receptor fragments also interfered with the ability of the wild-type V2 receptor to bind ligands. Toward this goal, membranes prepared from COS-7 cells coexpressing the wild-type V2 receptor and different V2 receptor truncation mutants were tested for their ability to bind the radioligand, [^{3}H]AVP. These studies showed that cotransfection of the Ni2, No2, and Ni3 constructs led to approximately 55−65% reductions in B_{max} values, as compared with vector-cotransfected control cells (175 ± 11 fmol/mg; set equal to 100% in each individual experiment) (Figure 5). However, [^{3}H]AVP K_D values determined in the presence of these three mutant constructs were similar to the value obtained with vector-cotransfected control cells (0.65 ± 0.12 nM; $n = 3$), and Scatchard analysis revealed the presence of single high-affinity [^{3}H]AVP binding sites (data not shown).

In contrast to the results obtained with the Ni2, No2, and Ni3 mutant receptors, coexpression of the Ni1 or No2 V2 receptor fragments had little or no effect on the [^{3}H]AVP binding properties of the wild-type receptor (Figure 5). Similarly, no reduction in maximum V2 receptor density (B_{max}) was observed with cells cotransfected with the wild-type V2 receptor and the V2-tail, m3-Ni3, or m3-tail receptor fragments (Figure 5).

TM I and II Are Not Required for the Dominant Negative Activity of Ni3. As outlined in the previous paragraphs, only

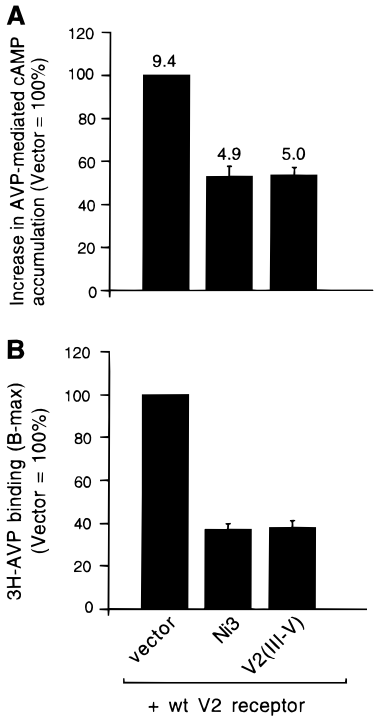

FIGURE 6: TM I and II are not required for the ability of Ni3 to inhibit wild-type V2 receptor function. COS-7 cells were cotransfected with plasmid DNA coding for the wild-type V2 receptor (0.25 μg) and the indicated mutant V2 receptor constructs or pcD-PS vector DNA (3.75 μg each). The structure of the Ni3 fragment is given in Figure 1. The V2(III−V) polypeptide was generated by deleting amino acids Arg38−Arg104 from Ni3, thus fusing the N-terminal extracellular segment of the V2 receptor to the middle of the o1 loop (Figure 1). (A) For cAMP assays, cells were incubated in 6-well plates for 30 min (at 37 °C) in the absence or presence of 1 μM AVP. The resulting increases in intracellular cAMP levels (fold stimulation above basal) were determined as described under Experimental Procedures. In each individual experiment, cAMP responses observed with vector-cotransfected control cells were set equal to 100%. Numbers above bars indicate actual increases in cAMP levels (fold stimulation above basal level; means). (B) [^{3}H]AVP binding studies were carried out with membrane homogenates prepared from cotransfected COS-7 cells as described under Experimental Procedures. Data are given as means ± SE of three independent experiments, each carried out in duplicate.

those mutant receptors that contained TM I−III (Ni2, No2, and Ni3) were able to act as negative regulators of wild-type V2 receptor function. To examine whether the presence of TM I and II was essential for the ability of V2 receptor fragments to inhibit V2 receptor activity, we created an additional expression construct coding for a V2 receptor polypeptide that included only TM III−V [V2(III−V)]. This construct was generated by deleting amino acids Arg38−Arg104 from Ni3, thus fusing the N-terminal extracellular segment of the V2 receptor to the middle of the o1 loop (Figure 1). Coexpression studies showed that the V2(III−V) polypeptide was able to inhibit V2 receptor-mediated cAMP production and [^{3}H]AVP binding in a fashion similar to the Ni3 fragment from which this polypeptide was derived (Figure 6).

Truncated V2 Receptors Reduce Cell Surface Expression of the Coexpressed Wild-Type V2 Receptor. Our next goal was to study whether truncated V2 receptors were able to interfere with proper cell surface localization of the coexpressed wild-type V2 receptor protein. To quantitate the amount of wild-type and mutant receptor proteins present on the cell surface, an indirect cellular ELISA was employed (*18*, *21*). For ELISA measurements, transfected COS-7 cells were incubated with the 12CA5 monoclonal antibody directed against the extracellular HA epitope tag present in all receptor constructs, followed by the addition of a peroxidase-conjugated secondary antibody and the photometric determination of peroxidase activity. Previous studies showed that this ELISA procedure does not interfere with the integrity of the plasma membrane barrier, as determined in control experiments with receptor constructs carrying C-terminal (intracellular) epitope tags (*18*).

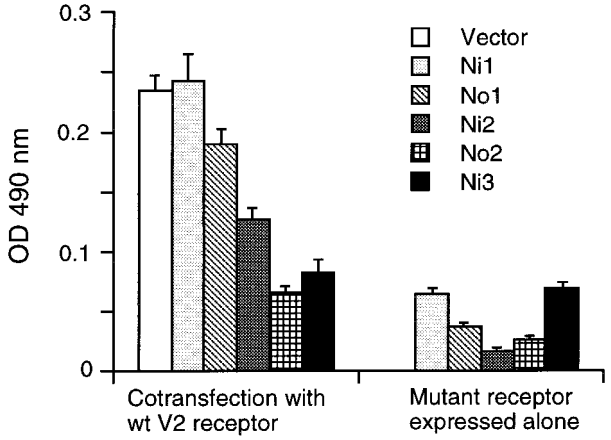

FIGURE 7: Reduction of cell surface expression of the wild-type V2 receptor by coexpressed truncated V2 receptors studied by ELISA. COS-7 cells were cotransfected with plasmid DNA coding for the wild-type V2 receptor (0.25 μg) and the indicated V2 mutant receptor constructs or pcD-PS vector DNA (3.75 μg each) (left panel). In another set of experiments (right panel), cells were transfected with truncated V2 receptor constructs alone (4 μg). ELISA measurements were carried out with intact COS-7 cells in 96-well plates as described under Experimental Procedures. All readings were corrected for background, determined with cells transfected with vector DNA alone (OD_{490nm} = 0.022 ± 0.003). Data are presented as means ± SE of three independent experiments, each carried out in quadruplicate.

Expression of the different V2 receptor truncation mutants alone resulted in rather weak OD signals (0.02−0.06), indicating that these mutant proteins were not well expressed on the cell surface (Figure 7). In contrast, expression of the wild-type V2 receptor construct resulted in a considerably more pronounced increase in OD readings (0.20−0.25). Strikingly, coexpression of the wild-type V2 receptor with the Ni2, No2, or Ni3 mutant constructs led to strong reductions in OD signals (by approximately 50−70%), as compared with vector-cotransfected control cells (Figure 7). Little or no reductions in OD readings were observed when the wild-type V2 receptor was cotransfected with the Ni1 and No1 receptor fragments.

Western Blot Analysis Reveals Dimeric Forms of Wild-Type and Mutant V2 Receptors. As outlined in the previous paragraphs, all V2 receptor truncation mutants capable of inhibiting wild-type V2 receptor function (Ni2, No2, and Ni3) also strongly interfered with cell surface expression of the coexpressed full-length V2 receptor. We therefore hypothesized that these mutant receptors are able to form complexes with the wild-type V2 receptor that are retained intracellularly in a nonfunctional state. To demonstrate that such interactions do in fact occur, we monitored protein expression more directly via Western blot analysis.

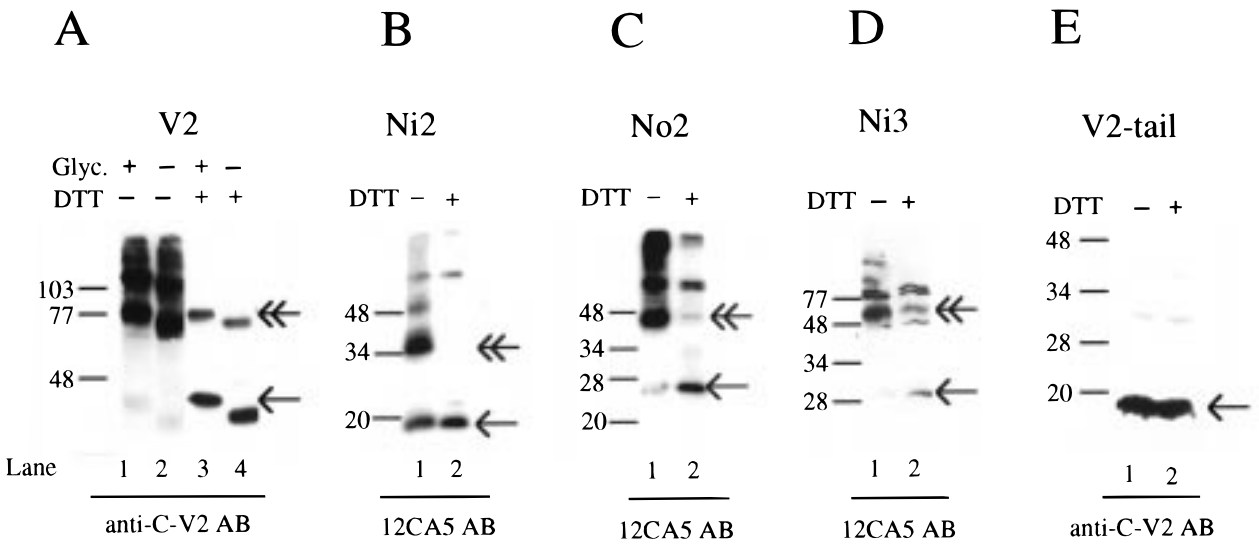

FIGURE 8: Detection of the wild-type V2 receptor and V2 receptor fragments via Western blot analysis. COS-7 cells were transfected with plasmid DNA (4 μg/dish) coding for the wild-type V2 receptor (A) and the indicated V2 receptor fragments (B−E) (for mutant receptor structures, see Figure 1). Membrane extracts were prepared about 70 h after transfections and subjected to SDS−PAGE (A, 10%; B−D, 12.5%; E, 15%) (10 μg of total protein/lane) as described under Experimental Procedures. Receptors/receptor fragments were visualized via immunoblotting using the anti-C-V2 polyclonal (A, E) or the 12CA5 (anti-HA) monoclonal antibody (B−D). Bands predicted to represent protein monomers are marked by a single arrow (→), while bands corresponding in size to putative receptor/fragment dimers are highlighted by a double arrow (→→). Immunoblotting experiments were also carried out with an Asn22→Gln mutant V2 receptor (A, lanes 2 and 4) that is no longer a substrate for N-linked glycosylation (Glyc-). To generate reducing conditions, samples were incubated with 100 mM DTT (final concentration) for 30 min at room temperature prior to SDS−PAGE. Please note that two nonspecific bands migrating at >80 kDa (which are also observed with mock-transfected cells; see Figure 9A, lane 6) are commonly seen upon use of the 12CA5 antibody (panels B−D). Protein molecular mass standards (in kDa) are indicated. Two additional experiments gave similar results.

Initially, we studied the expression of the wild-type V2 receptor protein when expressed alone. To detect the wild-type V2 receptor via immunoblotting, two different antibodies, the anti-C-V2 rabbit polyclonal antibody (raised against a peptide corresponding to the C-terminal 29 amino acids of the human V2 receptor) and the anti-HA 12C5A monoclonal antibody, were used (Figures 1, 8, and 9). Figure 8A shows a typical Western blot obtained with membrane lysates prepared from wild-type V2 receptor-expressing COS-7 cells, probed with the anti-C-V2 polyclonal antibody. Under nonreducing conditions, several different immunoreactive bands were observed (Figure 8A, lane 1): a faint band migrating at around 40 kDa, which corresponds in size to a putative receptor monomer, as well as several higher molecular mass forms that are likely to represent receptor dimers (at about 80 kDa) and oligomers (>100 kDa).

To further explore the possibility that the 80-kDa species in fact represents a V2 receptor dimer, immunoblotting experiments were also carried out with an Asn22→Gln V2 mutant receptor that is no longer a substrate for N-linked glycosylation (*27*). The pattern obtained with this glycosylation-defective mutant receptor was very similar to that obtained with the wild-type V2 receptor, except that the monomeric and dimeric forms were reduced in size by approximately 3−5 and 6−10 kDa, respectively (Figure 8A, lane 2). This observation is consistent with the notion that the 80-kDa band observed with the wild-type V2 receptor (Figure 8A, lane 1) does in fact represent a V2 receptor dimer.

When samples containing the wild-type V2 receptor protein (or the Asn22→Gln mutant receptor) were incubated with 100 mM DTT (room temperature, 30 min) prior to SDS−PAGE, the high-molecular mass products (>100 kDa) were no longer observed, and the putative dimer band became considerably weaker (Figure 8A, lanes 3 and 4). In contrast, the band corresponding to the putative V2 receptor monomer became very prominent. However, even after prolonged incubation (60 min at room temperature) of samples in the presence of very high concentrations of DTT (up to 200 mM) or β-mercaptoethanol (up to 5%) or heating of samples at 95 °C for 3 min (in the presence of 100 mM DTT), the signal corresponding to the V2 receptor dimer did not disappear completely (data not shown).

A pattern similar to that obtained with cells expressing the wild-type V2 receptor was also obtained with membrane lysates prepared from cells transfected with the Ni2, No2, and Ni3 mutant receptors (Figure 8B−D). On Western blots, the three polypeptides were detected with the 12CA5 monoclonal antibody directed against the N-terminal HA tag present in these as well as all other V2 receptor constructs. In each case, multiple immunoreactive bands were observed, including bands corresponding in size to fragment monomers and dimers. Upon treatment of samples with 100 mM DTT (room temperature, 30 min), most (Ni2, No2) or at least a substantial amount (Ni3) of the dimeric species were converted to the putative monomeric forms (Figure 8B−D).

In contrast to the findings obtained with the wild-type V2 and the Ni2, No2, and Ni3 mutant receptors, a different pattern was observed with membrane lysates prepared from cells expressing the V2-tail polypeptide. In immunoblotting experiments, the V2-tail fragment could be easily detected with the anti-C-V2 polyclonal antibody (Figure 8E). The V2-tail polypeptide, in contrast to the wild-type V2 and the Ni2, No2, and Ni3 mutant receptors, predominantly migrated as a monomer (approximate size, 16−18 kDa) both under nonreducing and reducing conditions (Figure 8E).

Western Blot Analysis Reveals the Formation of Heterodimers between Wild-Type and Truncated V2 Receptors.

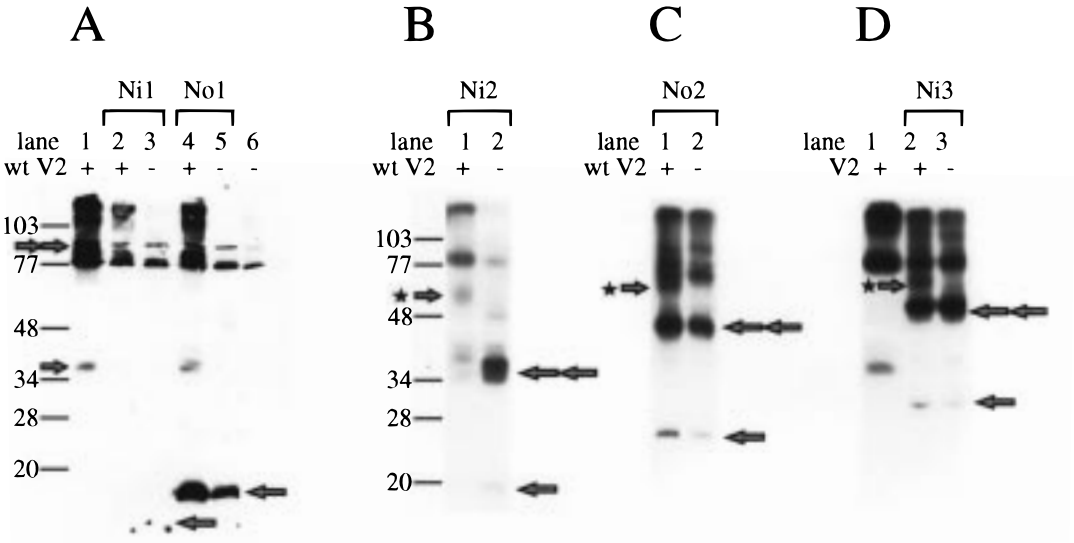

FIGURE 9: Formation of heterodimers between the wild-type V2 receptor and different V2 receptor truncation mutants, as detected by immunoblotting. COS-7 cells were transfected in 100-mm dishes with the following amounts of Ni1, No1, Ni2, No2, and Ni3 mutant receptor constructs, either alone or in combination with the wild-type V2 receptor plasmid (wt V2): (A) lane 1, wild-type V2 (4 μg); lane 2, wild-type V2 (0.75 μg) plus Ni1 (3.25 μg); lane 3, Ni1 (4 μg); lane 4, wild-type V2 (0.75 μg) plus No1 (3.25 μg); lane 5, No1 (4 μg); lane 6, mock-transfected cells. (B) lane 1, wild-type V2 (0.75 μg) plus Ni2 (3.25 μg); lane 2, Ni2 (4 μg). (C) lane 1, wild-type V2 (0.75 μg) plus No2 (3.25 μg); lane 2, No2 (4 μg). (D) lane 1, wild-type V2 (4 μg); lane 2, wild-type V2 (0.75 μg) plus Ni3 (3.25 μg); lane 3, Ni3 (4 μg). Membrane extracts were prepared about 70 h after transfections and subjected to nonreducing SDS−PAGE (A, 15%; B−D, 12%) (15 μg of total protein/lane), as described under Experimental Procedures. Receptors/receptor fragments were visualized by Western blotting using the 12CA5 (anti-HA) monoclonal antibody. Bands predicted to represent protein monomers are marked by a single arrow (→), bands corresponding in size to putative homodimers are highlighted by a double arrow (→→), and bands corresponding in size to putative wild-type/mutant receptor heterodimers are marked by an asterisk plus arrow (*→). Please note that several nonspecific bands migrating at >80 kDa (which are also observed with mock-transfected cells) are commonly seen upon use of the 12CA5 antibody. Protein molecular mass standards (in kDa) are indicated. Molecular mass markers were identical for panels B−D. Two additional experiments gave similar results.

We next wanted to examine whether the wild-type V2 receptor was able to form complexes with the different V2 receptor truncation mutants. Toward this goal, COS-7 cells were transfected with the Ni1, No1, Ni2, No2, and Ni3 mutant receptors, either alone or in combination with the wild-type V2 receptor (Figure 9). The 12CA5 anti-HA monoclonal antibody was used to detect these proteins via immunoblotting (under nonreducing conditions).

As shown in Figure 9A (lanes 3 and 5), analysis of membrane lysates prepared from Ni1- and No1-expressing cells led to the appearance of immunoreactive bands corresponding to monomeric fragment species (estimated molecular mass, 10 and 16 kDa, respectively); no polypeptide dimers were observed. In this set of experiments, the two bands migrating at around 80−90 kDa were caused by other cellular proteins cross-reacting with the 12CA5 antibody, since they were also observed using mock-transfected cells (Figure 9A, lane 6). Figure 9A also shows that the Ni1 signal was very weak, probably due to low expression and/or stability of this rather small receptor fragment (total size, 78 amino acids). No extra bands corresponding to heterodimeric complexes between wild-type V2 and the Ni1 or No1 mutant receptors were observed in coexpression experiments (Figure 9A, lanes 2 and 4).

Expression of the Ni2 receptor fragment alone resulted in the appearance of multiple immunoreactive bands, including bands corresponding in size to fragment monomers (at 17−19 kDa) and dimers (at 34−38 kDa) (Figure 9B, lane 2; see also Figure 8B). When Ni2 was coexpressed with the wild-type V2 receptor, an additional band of about 60 kDa appeared (Figure 9B, lane 1), consistent with the formation of heterodimers between wild-type V2 receptor and Ni2 fragment monomers. A pattern very similar to that found with the Ni2 mutant receptor was also observed with No2- and Ni3-expressing cells. In the case of No2, Western blot analysis again revealed several immunoreactive bands, including bands corresponding in size to monomeric (about 22−24 kDa) and dimeric (about 44−48 kDa) forms of No2 (Figure 9C, lane 2). Upon coexpression of No2 with the wild-type V2 receptor, an additional band, approximately 60−65 kDa in size, could be observed, probably representing a wild-type receptor/No2 heterodimer (Figure 9C, lane 1). Analogously, coexpression of the Ni3 truncation mutant with the wild-type V2 receptor also led to the appearance of a putative heterodimeric complex with a molecular mass of about 65−70 kDa (Figure 9D, lane 2). As observed with the Ni3 homodimer (Figure 8D), a considerable amount of the Ni3/wild-type V2 receptor heterodimer was converted to the monomeric species upon treatment of samples with 100 mM DTT (room temperature, 30 min) (data not shown). Coexpression of the wild-type V2 receptor with the m3-Ni3 mutant muscarinic receptor or coexpression of the wild-type rat V1a vasopressin receptor (*30*) with the Ni3 V2 receptor truncation mutant did not yield heterodimeric complexes in immunoblotting experiments (data not shown).

As shown in Figure 9, the V2 receptor monomer band (migrating at around 40 kDa) was not observed in the coexpression experiments, even when no heterodimers were detected, as in the case of Ni1. A likely explanation for this phenomenon is that expression of the wild-type V2 receptor protein is reduced in the coexpression experiments, probably due to competition between wild-type and mutant

receptor DNAs for amplification in COS-7 cells (please note that wild-type and mutant V2 receptor DNAs were not supplemented with vector DNA when their expression patterns were studied alone).

Analysis of the biochemical properties of a split rhodopsin mutant has shown that disulfide bond exchange reactions can occur when rhodopsin fragments are denatured in preparation for SDS−PAGE (*36*). To exclude such a mechanism as the molecular basis for the formation of heterodimeric complexes observed in Figure 9, cells coexpressing the wild-type V2 receptor and the Ni3 fragment were processed for SDS−PAGE (starting from the point of cell lysis) in the presence of the sulfhydryl alkylating reagent, *N*-ethylmaleimide (12.5 mM), as described by Kono *et al.* (*36*). The resulting pattern of immunoreactive bands was very similar to that shown in Figure 9D (lane 2) (data not shown), indicating that the formation of heterodimers is not an artifact due to disulfide bond exchange reactions during preparation of samples for SDS−PAGE.

DISCUSSION

In this study, we have tested the hypothesis that truncated GPCRs can act as negative regulators of wild-type receptor function. Toward this goal, we used the V2 vasopressin receptor, a prototypical G_S-coupled receptor, as a model system. Initially, the V2 receptor was split in the i3 loop, and the ability of the resulting receptor fragments, Ni3 and V2-tail (Figure 1), to modulate wild-type V2 receptor function was examined in cotransfected COS-7 cells. Whereas the C-terminal receptor polypeptide, V2-tail, failed to interfere with wild-type receptor activity, cells coexpressing the Ni3 fragment and the wild-type V2 receptor showed a strong reduction in AVP-dependent maximum cAMP responses (Figure 3). Increasing the amount of cotransfected Ni3 plasmid DNA led to a progressively more pronounced inhibition of the wild-type receptor signaling (Figure 2). The inability of the V2-tail polypeptide to affect wild-type receptor function is unlikely to be due to improper folding or membrane insertion, since we showed previously that coexpression of the Ni3 and V2-tail polypeptides results in the appearance of functional V2 receptor complexes (*21*). When the wild-type V2 receptor was coexpressed with a truncated rat m3 muscarinic receptor, m3-Ni3, which is structurally homologous to the Ni3 mutant V2 receptor (*17*), V2 receptor-mediated cAMP responses remained unaffected (Figure 3). This observation indicated that the ability of the Ni3 V2 mutant receptor to interfere with full-length V2 receptor function is specific for this receptor subtype.

To elucidate the minimum structural requirements for the ability of the Ni3 mutant receptor to serve as a negative regulator of wild-type V2 receptor function, we generated additional mutant V2 receptors that were truncated in the i1, o1, i2, and o2 loops (yielding Ni1, No1, Ni2, and No2, respectively). Coexpression studies showed that Ni2 and No2, like the Ni3 mutant receptor, strongly suppressed wild-type V2 receptor-mediated cAMP responses, whereas the Ni1 and No1 polypeptides were without effect (Figure 3). Thus, only those truncated receptors that contained the first three TM helices (TM I−III) displayed dominant negative activity. However, an Ni3-derived polypeptide that lacked TM I and II [referred to as V2(III−V)] was able to inhibit V2 receptor function in a fashion similar to Ni3 (Figure 6). This observation suggests that TM I and II are not required for the dominant negative activity of the V2 receptor fragments examined in this study and that TM III represents a major structural determinant mediating this activity.

Interestingly, studies with split m3 muscarinic receptors and rhodopsin have shown that fragments corresponding to Ni2, No2, and Ni3 (but not those homologous to Ni1 and No1) can form functional receptor complexes when coexpressed with the complimentary C-terminal receptor polypeptides (*17*−*20*). The Ni2, No2, and Ni3 receptor fragments can therefore be considered autonomous folding domains adopting a structure similar to that occurring in the full-length receptor.

In all coexpression experiments, effects observed with cells cotransfected with the wild-type V2 receptor construct and vector DNA served as control responses. Since only one protein (the wild-type receptor) is synthesized in this case, one might argue that the demands of making a second protein in the coexpression experiments may have led to reduced cAMP responses. However, the inability of the Ni1, No1, V2-tail, and m3 muscarinic receptor fragments to inhibit wild-type receptor function provided a useful internal control, indicating that cells cotransfected with the wild-type V2 receptor construct and vector DNA represented an adequate control.

To explore the molecular mechanisms underlying the ability of truncated V2 receptors to interfere with wild-type receptor function, several additional experiments were carried out. Previous studies with receptor fragments that included intracellular receptor sequences had shown that certain receptor-derived polypeptides can inhibit wild-type receptor function by sequestration of G proteins (*37*, *38*). To exclude such a mechanism as a potential cause for the dominant negative activity of truncated V2 mutant receptors, the Ni3 fragment was coexpressed with two other G_S-coupled receptors, the β2-adrenergic and the D1 dopamine receptors (Figure 4). These studies showed that the Ni3 protein, which strongly inhibited wild-type V2 receptor function, had no significant effect on maximum cAMP responses mediated by these two receptors. This observation suggested that the ability of Ni3 and other V2 receptor truncation mutants to act as negative regulators of wild-type V2 receptor function was not due to competition at the G protein level.

[^{3}H]AVP radioligand binding studies showed that the three V2 mutant receptors (Ni2, No2, and Ni3) that were capable of inhibiting V2 receptor-mediated cAMP formation also led to pronounced reductions in maximum [^{3}H]AVP binding sites (B_{max}) when coexpressed with the full-length receptor (Figure 5). Analogously, those receptor fragments that had little or no effect on V2 receptor signaling (Ni1, No1, and V2-tail) also had no major effect on the number of detected [^{3}H]-AVP binding sites. We therefore speculated that the Ni2, No2, and Ni3 mutant receptors interfere with mechanisms governing the proper delivery of the wild-type V2 receptor to the cell surface. To study cell surface receptor expression, we used an indirect cellular ELISA (*18*, *21*) employing a monoclonal antibody directed against an N-terminal (extracellular) HA epitope tag present in all wild-type and mutant V2 receptor constructs. These experiments showed that all truncated V2 receptors, in contrast to the wild-type V2 receptor, were poorly expressed on the cell surface (Figure

7). This observation is in agreement with previous studies indicating that truncation mutants (including Ni3) as well as many other mutant V2 receptors are largely retained intracellularly when expressed in cultured cells (*21, 39, 40*). However, we found, consistent with the results of the cAMP and radioligand binding assays, that cell surface expression of the wild-type receptor protein was considerably reduced upon coexpression with the No2, Ni2, and Ni3 mutant receptors (Figure 7).

On the basis of the ELISA results, we hypothesized that the Ni2, No2, and Ni3 fragments are able to form complexes with the full-length V2 receptor that are retained intracellularly in a nonfunctional state. To demonstrate that such interactions do in fact occur, we studied the expression of wild-type and mutant V2 receptors more directly via immunoblotting (Figures 8 and 9). When the wild-type V2 receptor was expressed alone, several immunoreactive bands were observed: a very faint band at around 40 kDa approximately corresponding to the size of the receptor monomer, and several higher molecular mass forms that are likely to represent receptor dimers and multimers. The pattern of bands observed with a glycosylation-defective V2 mutant receptor (carrying an Asn22→Gln point mutation; *27*) supported the concept that the 80-kDa wild-type receptor band in fact represents a V2 receptor dimer (Figure 8). When immunoblotting experiments were carried out under reducing conditions, the high molecular mass bands (>100 kDa) completely disappeared, the 80-kDa dimer band became considerably weaker, and the 40-kDa monomer became the predominant immunoreactive species, indicating that V2 receptor dimer/multimer formation involves intermolecular disulfide bonds.

Consistent with these findings, the ability of GPCRs to form SDS-resistant dimers/oligomers has been demonstrated recently for various GPCRs (*10*−*15*). Studies with β2-adrenergic (*10*) and D3 dopamine (*14*) receptors have shown that these oligomeric complexes are resistant to reducing agents. However, as observed here with the V2 vasopressin receptor, studies with mGluR5 glutamate (*12*) and CCR5 chemokine receptors (*15*) have also provided evidence for the existence of disulfide-linked GPCR dimers. In the case of the mGluR5 glutamate receptor, intermolecular disulfide bonds are formed between cysteine residues located in the extracellular N-terminal domain (*12*). The cysteine residues that play a role in the dimerization (oligomerization) of the V2 vasopressin receptor remain to be identified.

Immunoblotting experiments using membrane lysates prepared from cells expressing the Ni2, No2, and Ni3 mutant V2 receptors gave a pattern of immunoreactive bands resembling that found with wild-type receptor-expressing cells (nonreducing conditions): a weak band corresponding to the fragment monomer and several higher molecular mass bands corresponding in size to putative fragment dimers and multimers (Figure 9). On the other hand, fragments that failed to act as negative regulators of wild-type V2 receptor activity in the functional experiments (Ni1, No1, and V2-tail) were also unable to form polypeptide aggregates. The ability of mutant V2 receptors to interfere with wild-type V2 receptor function therefore strictly correlated with their ability to form dimeric/oligomeric complexes.

When the Ni2, No2, or Ni3 mutant receptors were coexpressed with the full-length V2 receptor, immunoblot analysis revealed the appearance of a novel immunoreactive species that was not observed with cells expressing the wild-type receptor or the truncation mutants alone (Figure 9). In all cases, the size of the novel band corresponded to the sum of wild-type and mutant receptor monomers, indicative of the formation of wild-type/mutant receptor heterodimers. No such heterodimeric species were observed when the Ni1, No1, and V2-tail fragments were coexpressed with the wild-type V2 receptor.

Taken together, these data are consistent with the notion that the ability of the Ni2, No2, and Ni3 mutant receptors to act as negative regulators of wild-type receptor function is due to the formation of wild-type/mutant receptor heterodimers that are retained intracellularly in a nonfunctional state. This notion is also supported by several recent studies that have examined the effect of other classes of mutant GPCRs on wild-type receptor function (*15*, *41*−*43*). Coexpression studies showed, for example, that a gonadotropin-releasing hormone receptor splice variant lacking TM VI and VII can interfere with wild-type receptor-mediated inositol phosphate accumulation, probably by preventing proper cell surface localization of the full-length receptor protein (*41*). Interestingly, a naturally occurring mutation in the CCR5 chemokine receptor (which functions as a co-receptor for HIV-1 entry) coding for a mutant receptor truncated in the o2 loop (ccr5Δ32) has been shown to provide relative protection from AIDS (*42*). When CCR5 wild-type and ccr5Δ32 mutant receptors were coexpressed in the same cell, immunocytochemical studies revealed that cell surface expression of the wild-type receptor was significantly reduced (*15*). Finally, Zucker and coworkers recently isolated a series of rhodopsin mutants that act dominantly to cause retinal degeneration in *Drosophila* (*43*). Biochemical studies showed that the mutant rhodopsin proteins cause retinal degeneration by interfering with the maturation of wild-type rhodopsin (*43*). Taken together, these findings support the concept that GPCRs can form oligomeric arrays and that improperly folded mutant receptors can interfere with the proper function/intracellular trafficking of such complexes.

The molecular mechanisms involved in the formation of heterodimers between wild-type and mutant V2 vasopressin receptors (or other GPCRs) remain unclear at present. Since heterodimer formation strictly correlates with the ability of the mutant receptors to form homodimers, similar molecular interactions appear to be involved in both processes. Hebert *et al.* (*10*) recently showed that a peptide corresponding to TM VI of the β2-adrenergic receptor inhibits β2-receptor dimerization, suggesting that TM VI represents part of the receptor surface critical for dimerization. Another study found that dimerization of the δ opioid receptor critically depends on the presence of the C-terminal 15 amino acids of the receptor protein (*13*). However, the dominant negative V2 receptor truncation mutants identified in this study (Ni2, No2, and Ni3) all lack TM VI as well as other C-terminal sequences, suggesting that V2 receptor dimerization/heterodimer formation involves a different structural mechanism. Heterodimer formation between wild-type and mutant V2 receptors appears to be a rather specific process, since no such complexes were observed upon coexpression of the full-length V2 receptor and a truncated rat m3 muscarinic receptor (m3-Ni3) that is structurally homologous to the Ni3 mutant V2 receptor (data not shown). On the basis of current

ideas about the folding of polytopic transmembrane proteins (*44*), it seems reasonable to assume that helix−helix interactions are likely to be involved in receptor dimer/heterodimer formation. The molecular identity of such interactions remains to be elucidated.

Besides their usefulness as research tools to dissect GPCR-mediated signal transduction pathways, mutant receptors or receptor fragments displaying dominant negative activity are also of potential therapeutic interest. It has been shown during the past few years that a variety of human diseases are caused by activating mutations in distinct GPCRs (constitutively active GPCRs; *45*). It is conceivable that expression of polypeptides displaying dominant negative activity will be of therapeutic benefit by reducing basal signaling of such mutant GPCRs.

Mutant V2 receptors are also known to be of considerably pathophysiologic relevance. Several laboratories have shown (for a recent review, see ref *46*) that mutations in the V2 vasopressin receptor gene (including single codon changes as well as nonsense and frame-shift mutations leading to truncated receptor proteins) are responsible for X-linked NDI, a disease characterized by the inability of the kidney to concentrate urine. Although this disease is primarily observed in males, several female carriers of mutant V2 receptor alleles (including alleles coding for truncated receptor proteins) have been described who display an NDI phenotype (*47*−*49*). Since one of the two X-chromosomes in females is silenced in mammals ('X-inactivation'; ref *50*), it is unlikely that wild-type and mutant V2 receptor proteins are expressed in the same cell. It has therefore been proposed (*47*−*49*) that 'skewed' X-inactivation (resulting in the predominant inactivation of the wild-type V2 receptor allele) rather than dominant negative inhibition of wild-type receptor function by mutant V2 receptors is responsible for the NDI phenotype observed in females carrying mutant V2 receptor alleles.

In summary, we have shown that truncated V2 receptors containing at least three TM domains can act as negative regulators of wild-type receptor function. The dominant negative activity of these mutant receptors strictly correlated with their ability to reduce cell surface expression of the wild-type receptor protein and to form heterodimeric complexes with the full-length V2 receptor, strongly suggesting that the ability of these mutant receptors to interfere with wild-type receptor function is due to direct protein−protein interactions. Since all GPCRs share a similar molecular architecture and mechanism of action, our results should be of broad general relevance.

ACKNOWLEDGMENT

We thank Drs. M. Brownstein and C. M. Fraser for generously providing us with receptor expression plasmids and Drs. F.-Y. Zeng and E. Kostenis for helpful discussions.

REFERENCES

1. Dohlman, H. G., Thorner, J., Caron, M. G., and Lefkowitz, R. J. (1991) *Annu. Rev. Biochem. 60*, 653−688.
2. Strader, C. D., Fong, T. M., Tota, M. R., Underwood, D., and Dixon, R. A. F. (1994) *Annu. Rev. Biochem. 63*, 101−132.
3. Watson, S., and Arkinstall, S. (1994) in *The G-Protein Linked Receptor—Facts Book* (Watson, S., and Arkinstall, S., Eds.) pp 1−291, Academic Press, London.
4. Potter, L. T., Ballesteros, L. A., Bichajian, L. H., Ferrendelli, C. A., Fisher, A., Hanchett, H. E., and Zhang, R. (1991) *Mol. Pharmacol. 39*, 211−221.
5. Hirschberg, B. T., and Schimerlik, M. I. (1994) *J. Biol. Chem. 269*, 26127−26135.
6. Wreggett, K. A., and Wells, J. W. (1995) *J. Biol. Chem. 270*, 22488−22499.
7. Chidiac, P., Green, M. A., Pawagi, A. B., and Wells, J. W. (1997) *Biochemistry 36*, 7361−7379.
8. Maggio, R., Vogel, Z., and Wess, J. (1993) *Proc. Natl. Acad. Sci. U.S.A. 90*, 3103−3107.
9. Monnot, C., Bihoreau, C., Conchon, S., Curno, K. M., Corvol, P., and Clauser, E. (1996) *J. Biol. Chem. 271*, 1507−1513.
10. Hebert, T. E., Moffett, S., Morello, J.-P., Loisel, T. P., Bichet, D. G., Barret, C., and Bouvier, M. (1996) *J. Biol. Chem. 271*, 16384−16392.
11. Ng, G. Y. K., O'Dowd, B. F., Lee, S. P., Chung, H. T., Brann, M. R., Seeman, P., and George, S. R. (1996) *Biochem. Biophys. Res. Commun. 227*, 200−204.
12. Romano, C., Yang, W.-L., and O'Malley, K. L. (1996) *J. Biol. Chem. 271*, 28612−28616,
13. Cvejic, S., and Devi, L. A. (1997) *J. Biol. Chem. 272*, 26959−26964.
14. Nimchinsky, E. A., Hof, P. R., Janssen, W. G. M., Morrison, J. H., and Schmauss, C. (1997) *J. Biol. Chem. 272*, 29229−29237.
15. Benkirane, M., Jin, D.-Y., Chun, R. F., Koup, R. A., and Jeang, K.-T. (1997) *J. Biol. Chem. 272*, 30603−30606.
16. Kobilka, B. K., Kobilka, T. S., Daniel, K., Regan, J. W., Caron, M. G., and Lefkowitz, R. J. (1988) *Science 240*, 1310−1316.
17. Maggio, R., Vogel, Z., and Wess, J. (1993) *FEBS Lett. 319*, 195−200.
18. Schöneberg, T., Liu, J., and Wess, J. (1995) *J. Biol. Chem. 270*, 18000−18006.
19. Ridge, K. D., Lee, S. S. J., and Yao, L. L. (1995) *Proc. Natl. Acad. Sci. U.S.A. 92*, 3204−3208.
20. Yu, H., Kono, M., McKee, T. D., and Oprian, D. D. (1995) *Biochemistry 34*, 14963−14969.
21. Schöneberg, T., Yun, J., Wenkert, D., and Wess, J. (1996) *EMBO J. 15*, 1283−1291.
22. Birnbaumer, M., Seibold, A., Gilbert, S., Ishido, M., Barberis, C., Antaramian, A., Brabet, P., and Rosenthal, W. (1992) *Nature 357*, 333−335.
23. Higuchi, R. (1989) in *PCR Technology* (Erlich, H. A., Ed.) pp 61−70, Stockton Press, New York.
24. Kolodziej, P. A., and Young, R. A. (1991) *Methods Enzymol. 194*, 508−519.
25. Liu, J., and Wess, J. (1996) *J. Biol. Chem. 270*, 8772−8778.
26. Wildin, R. S., Antush, M. J., Bennett, R. L., Schoof, J. M., and Scott, C. R. (1994) *Am. J. Hum. Genet. 55*, 266−277.
27. Innamorati, G., Sadeghi, H., and Birnbaumer, M. (1996) *Mol. Pharmacol. 50*, 467−473.
28. Zhou, Q. Y., Grandy, D. K., Thambi, L., Kushner, J. A., Van Tol, H. H., Cone, R., Pribnow, D., Salon, J., Bunzow, J. R., and Civelli, O. (1990) *Nature 347*, 76−80.
29. Gocayne, J., Robinson, D. A., Fitzgerald, M. G., Chung, F.-Z., Kerlavage, A. R., Lentes, K.-U., Lai, J., Wang, C.-D., Fraser, C. M., and Venter, J. C. (1987) *Proc. Natl. Acad. Sci. U.S.A. 84*, 8296−8300.
30. Morel, A., O'Carroll, A.-M., Brownstein, M. J., and Lolait, S. J. (1992) *Nature 356*, 523−526.
31. Cullen, B. R. (1987) *Methods Enzymol. 152*, 684−704.
32. Dörje, F., Wess, J., Lambrecht, G., Tacke, R., Mutschler, E., and Brann, M. R. (1991) *J. Pharmacol. Exp. Ther. 256*, 727−733.
33. Bradford, M. M. (1976) *Anal. Biochem. 72*, 248−254.
34. Munson, P. J., and Rodbard, D. (1980) *Anal. Biochem. 107*, 220−239.
35. Salomon, Y., Londos, C., and Rodbell, M. (1974) *Anal. Biochem. 58*, 541−548.
36. Kono, M., Yu, H., and Oprian, D. D. (1998) *Biochemistry 37*, 1302−1305.
37. Luttrell, L. M., Ostrowski, J., Cotecchia, S., Kendall, H., and Lefkowitz, R. J. (1993) *Science 259*, 1453−1457.

38. Hawes, B. E., Luttrell, L. M., Exum, S. T., and Lefkowitz, R. J. (1994) *J. Biol. Chem. 269*, 15776−15785.
39. Tsukaguchi, H., Matsubara, H., Taketani, S., Mori, Y., Seido, T., and Inada, M. (1995) *J. Clin. Invest. 96*, 2043−2050.
40. Sadeghi, H. M., Innamorati, G., and Birnbaumer, M. (1997) *Mol. Endocrinol. 11*, 706−713.
41. Grosse, R., Schöneberg, T., Schultz, G., and Gudermann, T. (1997) *J. Mol. Endocrinol. 11*, 1305−1318.
42. Samson, M., Libert, F., Doranz, B. J., Rucker, J., Liesnard, C., Farber, C.-M., Saragosti, S., Lapoumeroulie, C., Cognaux, J., Forceille, C., Muyldermans, G., Verhofstede, C., Burtonboy, G., Georges, M., Imai, T., Rana, S., Yi, Y., Smyth, R. J., Collman, R. G., Doms, R. W., Vassart, G., and Parmentier, M. (1996) *Nature 382*, 722−725.
43. Colley, N. J., Cassill, J. A., Baker, E. K., and Zuker, C. S. (1995) *Proc. Natl. Acad. Sci. U.S.A. 92*, 3070−3074.
44. Popot, J.-L., and Engelman, D. M. (1990) *Biochemistry 29*, 4031−4037.
45. Spiegel, A. M. (1996) *Annu. Rev. Physiol. 58*, 143−170.
46. Birnbaumer, M. (1995) *J. Rec. Sign. Transduct. Res. 151*, 131−160.
47. Van Lieburg, A. F., Verdijk, M. A. J., Schoute, F., Ligtenberg, M. J. L., van Oost, B. A., Waldhauser, F., Dobner, M., Monnens, L. A. H., and Knoers, N. V. A. M. (1995) *Hum. Genet. 96*, 70−78.
48. Moses, A. M., Sangani, G., and Miller, J. L. (1995) *J. Clin. Endocrinol. Metab. 80*, 1184−1186.
49. Nomura, Y., Onigata, K., Nagashima, T., Yutani, S., Mochizuki, H., Nagashima, K., and Morikawa, A. (1997) *J. Clin. Endocrinol. Metab. 82*, 3434−3437.
50. Migeon, B. R. (1994) *Trends Genet. 10*, 230−235.

BI981162Z